

## Whole-body magnetic resonance imaging for detection of malignant disease: A head-to-head-comparison with whole-body <sup>18</sup>F-FDG-PET/CT as the reference standard

Lau Brix<sup>1,2,\*</sup> MSc, PhD, June Anita Ejlersen<sup>3</sup> MD, PhD, Joan Fledelius<sup>3</sup> MD, PhD, Inga Makieva<sup>1</sup> MD, Erik Sven Göran Thylin<sup>1</sup> MD, John Hansen<sup>1</sup> BSc, Liam Kieu Ha<sup>1</sup> BSc, Oke Gerke<sup>4</sup> PhD and Christin Isaksen<sup>1</sup> MD

<sup>1</sup>Department of Radiology, Diagnostic Centre, University Research Clinic for Innovative Patient Pathways, Silkeborg Regional Hospital, Denmark

<sup>2</sup>Department of Procurement and Clinical Engineering, Region Midt, Denmark

<sup>3</sup>Department of Nuclear Medicine, Herning Regional Hospital, Denmark

<sup>4</sup>Department of Nuclear Medicine, Odense University Hospital, Odense, Denmark

### Abstract

**Introduction:** The combined use of <sup>18</sup>F-FDG-PET and computed tomography (CT) scans is an integrated part of diagnosing and staging patients with suspected malignancy or other pathologies. Magnetic resonance imaging (MRI) has proven its use as a non-ionizing imaging alternative for identifying potential malignancy in specific organs. **Objective:** To investigate the clinical value of whole-body MRI in detection of suspicious lesions, we compared 1.5T MRI findings to those obtained from a whole-body <sup>18</sup>F-FDG-PET/CT scan, the latter serving as the reference standard. Finally, the findings were compared with histology if available. **Materials and methods:** Twenty-five patients (9 women and 16 men, mean age ± SD: 64.5 ± 11.8 years; range: 34±85 years) with suspected malignancy or other pathologies were enrolled. All patients were scanned using both modalities. Imaging included the head, torso and extremities. Images were scored blinded by experienced readers: two radiologists and two nuclear medicine physicians. Statistical tests included weighted kappa for measuring interobserver reliability and Wilcoxon signed-rank test for detection differences between paired observations. **Results and discussion:** Interobserver reliability between each pair of specialists was fair-to-strong (Weighted kappa). Statistically significant differences between the findings of the two modalities were found in the colon (p=0.016), soft tissues of the extremities (p=0.002) and skeleton of the extremities (p=0.008). Twelve patients had histology available. WB-MRI and whole-body <sup>18</sup>F-FDG-PET/CT found 10 of these cases (sensitivity: 83.3%, 95% CI: 55.2%-95.3%). **Conclusion:** The diagnostic value of WB-MRI equaled whole-body <sup>18</sup>F-FDG-PET/CT. The MRI approach could therefore be considered in patients unsuitable for <sup>18</sup>F-FDG-imaging e.g. younger patients, during pregnancy or dysregulated diabetics.

**Keywords:** diffusion-weighted MRI; malignant disease; suspicious lesion detection; <sup>18</sup>F-FDG avid foci; occult cancer

### Introduction

First line examinations when malignant disease or other pathologies (e.g. inflammation or infectious disease) are suspected include clinical evaluation, biochemical tests, X-ray, ultrasound and computed tomography (CT). Fluorine-18 fluorodeoxyglucose positron emission tomography combined with low dose non-contrast-enhanced CT (<sup>18</sup>F-FDG-PET/CT) may be added to the examination repertoire to stage and characterize potential pathological lesions further. The results are used for planning the subsequent treatment as the modality is highly sensitive for clarification of staging, prognosis and response to therapy [1-4]. Furthermore, the <sup>18</sup>F-FDG-PET/CT modality is useful in staging malignancies in the breast, colorectal, head and neck, lung, lymphoma, melanoma, esophageal and thyroid or detection of an unknown primary tumor [5].

Inherent challenges of the <sup>18</sup>F-FDG-PET/CT hybrid modality may cause diagnostic challenges, such as misregistration artifacts when merging CT and PET images [6]. Furthermore, <sup>18</sup>F-FDG uptake is not specific for malignant lesions versus

other pathologies and the results may be hampered by physiologic variations of nuclear tracer accumulation. Conversely, false-negative results may be seen in low-grade tumors as they exhibit slow metabolic rates [7].

Non-ionizing whole-body magnetic resonance imaging (WB-MRI) could be an alternative or supplement to the nuclear

**\*Corresponding author:** Lau Brix, Department of Radiology, Diagnostic Centre, Silkeborg Regional Hospital, Region Midt, Falkevej 1-3, DK-8600 Silkeborg, Denmark. Tel.: +45 7841 7500; Fax: +45 7841 4580; Email: [lau.brix@rm.dk](mailto:lau.brix@rm.dk)

Received 23 January 2019 Revised 14 March 2020 Accepted 20 March 2020  
Published 30 March 2020

**Citation:** Brix L, Ejlersen JA, Fledelius J, Makieva I, Thylin ESG, Hansen J, Ha LK, Gerke O, Isaksen C. Whole-body magnetic resonance imaging for detection of malignant disease: A head-to-head-comparison with whole-body <sup>18</sup>F-FDG-PET/CT as the reference standard. J Radiol Imaging. 2020; 4(3):17-24. DOI: [10.14312/2399-8172.2020-3](https://doi.org/10.14312/2399-8172.2020-3)

**Copyright:** © 2020 Brix L, et al. Published by NobleResearch Publishers. This is an open-access article distributed under the terms of the [Creative Commons Attribution License](https://creativecommons.org/licenses/by/4.0/), which permits unrestricted use, distribution and reproduction in any medium, provided the original author and source are credited.

based imaging approach [8-12]. Studies have shown that information on tumor burden and tumor spreading can be obtained from MRI without the use of a contrast agent [13, 14], hence MRI is useful in identifying malignancies or other pathologies in specific organs, but the ability to screen the entire body, such as  $^{18}\text{F}$ -FDG-PET/CT remains to be elucidated. We hypothesized that WB-MRI could be a radiation friendly screening alternative to  $^{18}\text{F}$ -FDG-PET/CT for identifying potential suspicious lesions in organs, soft tissues, lymph nodes and/or the skeleton. In this context, MRI suspicious lesions are defined as focal areas of high signal on MRI identified on the WB-DWI images ( $b=900\text{ s/mm}^2$ ) with low signal correlation on ADC map.

The purpose of the study was to investigate the diagnostic value of WB-MRI with  $^{18}\text{F}$ -FDG-PET/CT as the reference method. In a subgroup of patients with an inconclusive CT scan, histology served as the reference method for both modalities (MRI and  $^{18}\text{F}$ -FDG-PET/CT).

## Materials and methods

### Patient group

All included patients were referred to a  $^{18}\text{F}$ -FDG-PET/CT scan due to inconclusive findings on a preliminary diagnostic CT scan suspicious for malignancy or other pathologies (e.g. inflammation or infection). Patients with prior malignant disease were excluded from the study. Patient inclusion was carried out during a one-year period (August 2014 to August 2015). Twenty-five patients were included in the study (9 women and 16 men, mean age  $\pm$  standard deviation:  $64.5 \pm 11.8$  years; range: 34–85 years). None of the patients received anti-diabetic drugs as this may have influenced the sensitivity of the  $^{18}\text{F}$ -FDG-PET/CT especially in the abdomen. The study was approved by the local ethical committee (case no. 1-10-72-381-13) and all enrolled patients gave their written consent.

### MRI techniques

All MRI scans were carried out on a Siemens Avanto 1.5T MRI scanner (software release VB17a Siemens Healthcare GmbH, Erlangen, Germany). The patients were placed in the supine position and entered the bore head first with their arms placed by their sides. MRI signal detection was done with dedicated receive coils that covered the entire scan area from head to toes. The imaging protocols were divided into two areas of interest. One aimed specifically at the whole-spine (bones, intervertebral discs, spinal cord and cerebrospinal fluid) using sagittal slice planes while the other targeted the whole-body (organs, soft tissues and lymph nodes) using axial slice planes. No contrast agent was administered for the MRI examinations.

The whole-spine sequences consisted of a sagittal 2D  $T_1$ -weighted fast spin-echo sequence (two imaging stations covering C0-S2, TR = 400-519 ms, TE = 10-11 ms, slice spacing = 0.4 mm, bandwidth = 161-200 Hz, Echo train length = 3-4, field of view = 380-420 $\times$ 380-420 mm, matrix size = 240-278 $\times$ 320, slice thickness = 4 mm, flip angle = 150°) and a sagittal 2D  $T_2$ -weighted fast spin-echo with fat saturation (two imaging stations, TR = 3960-4350 ms, TE = 78 ms, slice spacing = 0.4 mm, bandwidth = 191 Hz, Echo train length = 16-18, field of view = 380-420 $\times$ 380-420 mm,

matrix size = 240 $\times$ 320, slice thickness = 4 mm, flip angle = 150°).

The whole-body sequences consisted of an axial DWIBS (Diffusion-weighted whole-body imaging with body background signal suppression) sequence (eight stations with complete anterior to posterior coverage from vertex to toes, TR = 9000 ms, TE = 68 ms, TI = 180 ms, bandwidth = 1628 Hz, Number of Signal Averages = 4, Field of view = 500 $\times$ 500 mm, matrix size = 204 $\times$ 256, slice thickness = 5 mm, flip angle = 90°, b-values = 50 and 900  $\text{s/mm}^2$ ) and an axial 2D  $T_1$ -weighted fast spin-echo sequence (five imaging stations, TR = 410-700 ms, TE = 8.6-9.4 ms, bandwidth = 178-217 Hz, Echo train length = 2-6, field of view = 250-400 $\times$ 500 mm, matrix size = 192 $\times$ 384, slice thickness = 5 mm, flip angle = 90°).

Apparent diffusion coefficient (ADC) maps were calculated ( $b=50\text{ s/mm}^2$  and  $b=900\text{ s/mm}^2$ ) to evaluate possible  $T_2$ -shine-through effects. Diffusion images were re-sliced to the coronal slice plane and contrast inverted to resemble the nuclear based scans.

### $^{18}\text{F}$ -FDG-PET/CT techniques

All  $^{18}\text{F}$ -FDG-PET/CT scans were carried out on a Siemens Biograph mCT 4R-64 slice PET/CT scanner (Siemens Healthcare GmbH, Erlangen, Germany). The patients were placed in the supine position with their arms placed above their heads. Patients were instructed to fast for at least 6 h prior to the  $^{18}\text{F}$ -FDG injection. A dose of  $^{18}\text{F}$ -FDG (4MBq/kg) was administered intravenously into a cubital vein, after which the scans were obtained 60 $\pm$ 5 min post injection (30 min resting in bed and 30 min resting while sitting prior to scanning). The  $^{18}\text{F}$ -FDG-PET/CT scans were performed by initially obtaining a whole-body low dose CT scan (slice width 2.0 mm, collimation 64 $\times$ 0.6 mm, pitch 1.2 and rotation time 0.5 seconds, using dose modulation for both mAs (Quality reference mAs 50, effective mAs 120) and voltage (ref. 120 KV; allowed range 100–140 KV)). This was followed by a whole-body  $^{18}\text{F}$ -FDG-PET scan to ensure that the same anatomical area as the MRI examination was imaged (21 cm axial field of view, typically 12-15 bed positions depending on patient-height, with acquisition times of 2-3 min/bed-position depending on patient BMI; a typical scan being 3 min/bed-position over the head, torso and abdomen, with a reduction to 2 min/bed-position over the lower extremities).

Postprocessing of the CT-data was performed using two axial iterative reconstructions: one to perform attenuation correction of the  $^{18}\text{F}$ -FDG-PET-data (2 mm slice thickness, extended field of view (780 mm), B30f medium smooth kernel) and the other for fusion with the PET images to perform localization and characterization evaluation of the uptake in the PET images (2 mm slice thickness, 500 mm field of view, safire strength 3, I30f medium smooth kernel).

Postprocessing of the  $^{18}\text{F}$ -FDG-PET images were iteratively reconstructed using both attenuation and scatter correction, and ultra-high definition PET: Siemens True X, time-of-flight and point spread function corrections were

applied (2 iterations/21 subsets, matrix size = 400, zoom 1, 2mm gauss filter and 2mm slice thickness).

#### Data evaluation

Two experienced MRI radiologists and two experienced nuclear medicine physicians evaluated the MRI and  $^{18}\text{F}$ -FDG-PET/CT images using a standardized form. MRI images were evaluated using a standard clinical PACS system (Agfa IMPAX version 6.5 Agfa Healthcare NV, Mortsel, Belgium), and  $^{18}\text{F}$ -FDG-PET/CT images were evaluated using a dedicated workstation (Siemens syngo.via Workplace MI, Siemens Healthcare GmbH, Erlangen, Germany).

The observers were instructed to count the number of suspicious lesions/ $^{18}\text{F}$ -FDG avid foci found in the lymph nodes (collum, axilla, mediastinum, lungs, abdomen, pelvis and inguinal), the organ systems (cerebrum, extra cerebral, collum, lungs and pleura, mediastinum, hepar, vesica fellea, spleen, renes, adrenals, pancreas, genitalia interna and vesica urinariae), the gastrointestinal tract (oesophagus, ventriculus, intestinum, colon and mesenterium), the soft tissues (collum, thorax, abdomen, pelvis and extremities) and the skeleton (cranium and faciem, columna, thorax, pelvis and extremities). MRI suspicious lesions were identified on the WB-DWI images ( $b=900\text{ s/mm}^2$ ) with ADC map correlation and compared to the morphological MRI images in respect to anatomy, localization, size and the preexisting CT scan.

$^{18}\text{F}$ -FDG-PET/CT lesions (FDG avid foci) were identified visually as having an  $^{18}\text{F}$ -FDG uptake appreciably higher than the surrounding background to keep the sensitivity as high as possible. For both modalities, all findings were noted on a 4-point scale. A 0 was assigned when no lesion was detected, a 1 was assigned when one lesion was detected, a 2 was assigned when two lesions were detected and 3 whenever three or more lesions were detected. The 4-point scale was chosen for several reasons. It was important to distinguish between no lesion (0) and the presence of lesions in individual organs (1-3). Thus, the most important step on the scale is from 0-1, while 2-3 was used to give the four reviewers (radiologists and nuclear physicians) the opportunity to indicate the severity of lesions in a given organ.

#### Histological findings

The combined results from the  $^{18}\text{F}$ -FDG-PET/CT scans and the clinical examinations led to biopsies at specific locations in some of the patients. Due to logistics, not all suspicious lesions identified by either  $^{18}\text{F}$ -FDG-PET/CT and/or WB-MRI were supported by biopsies. If histology was obtained, this information served as the ground truth when comparing the two modalities. These results were compared at patient level.

#### Statistics

Descriptive statistics comprised mean  $\pm$  standard deviation and range. Weighted kappa statistics with linear weights were used for measuring interobserver reliability on each of the two modalities [15, 16]. The kappa values were supported by Wald-type 95% confidence intervals (95% CIs). These tests were used to compare the number of MRI

suspicious lesions and FDG avid foci (0-3) found between raters of the WB-MRI and  $^{18}\text{F}$ -FDG-PET/CT examinations respectively. Weighted kappa values were interpreted as being poor ( $<0.0$ ), slight (0.0-0.20), fair (0.21 - 0.40), moderate (0.41 - 0.60), substantial (0.61 - 0.80) and almost perfect (0.81 - 1.00) [17]. Patient-based sensitivity for both modalities was assessed based on available histology and supplemented by Wilson-score 95% CIs [18].

Differences between the paired observations (WB-MRI vs.  $^{18}\text{F}$ -FDG-PET/CT) were done using two-sided Wilcoxon signed-rank tests and  $p$  values  $\leq 0.05$  were considered to be statistically significant. In order to do this, we used a worst-case consensus approach in which the reviewer with the highest number of noted suspicious lesions/ $^{18}\text{F}$ -FDG avid foci in each unique anatomical region was used for the statistical analysis.

The time between the two examinations, the total scan time used for scanning (scan preparation and time spent in each scanner), the time used by each observer for evaluation of the image data and the total radiation dose were also noted. All observers were blinded to the findings of the other raters.

In order to detect a paired difference in the classified findings (0 to 3) between the two examinations of one with a standard deviation of 1.6, a sample size of 23 was needed (power: 80%, significance level: 5%). To account for drop-outs, we therefore included a total of 25 patients in the study. All statistical analyses were performed in Microsoft Excel 2016 with the statistical add-in tool pack Analyse-It<sup>®</sup> (Version 4.65.3, Analyse-it Software Ltd, Leeds, England).

## Results

Interobserver reliability analysis between the two MRI radiologists yielded weighted kappa values of 0.26–0.90 while the nuclear physicians yielded values of 0.26–0.88, implicating fair to strong reliability in both modalities. The Wilcoxon Signed-rank tests found statistically significant differences in the colon ( $p=0.016$ ) the soft tissue of the extremities ( $p=0.002$ ) and in the skeleton of the extremities ( $p=0.008$ ). All statistical data can be found in Table 1.

Histological tests were performed in 12 of the 25 patients. Table 2 shows the histological findings of primary cancer and the complimentary findings using the two modalities. Discrepancies between modalities were found in two patients (Patient #3 and #13) which both had prostate cancer. One of them was identified by  $^{18}\text{F}$ -FDG-PET/CT and not WB-MRI while the other was identified by only one of the MRI radiologists and neither of the nuclear medical physicians. Finally, both modalities missed a renal cell carcinoma (Patient#14). Assessing conservatively positivity whenever at least one MRI radiologist or one nuclear medical physician did so lead to a sensitivity for both MRI and PET/CT of 83.3% (95% CI: 55.2-95.3).

The average time between the WB-MRI and  $^{18}\text{F}$ -FDG-PET/CT examinations was  $3.8\pm 3.1$  days (range: 0-12 days). The mean preparation time for the WB-MRI and  $^{18}\text{F}$ -FDG-PET/CT examinations were  $12.6 \pm 3.1$  min and  $10 \pm 0.0$  min, while the total scan time were  $75.5 \pm 9.6$  min and 31.6

**Table 1** Statistical calculations for hot spot lesion detection using whole body MRI and <sup>18</sup>F-FDG-PET/CT. Weighted kappa for interobserver reliability between two radiologists (MRI) and two nuclear medicine physicians. Two-sided Wilcoxon signed-rank tests were used to detect differences between paired observation (MRI vs. <sup>18</sup>F-FDG-PET/CT).

Anatomy	Weighted kappa, $\kappa_w$		Wilcoxon signed-rank
	MRI	<sup>18</sup> F-FDG-PET/CT	MRI vs. <sup>18</sup> F-FDG-PET/CT
<i>Lymph nodes</i>	$\kappa_w$ (95% CI <sup>a</sup> )	$\kappa_w$ (95% CI)	<i>p</i> -value
Throat	0.53 (0.26-0.80)	0.80 (0.61-0.98)	0.81
Axils	0.81 (0.60-1.00)	0.62 (0.30-0.93)	0.19
Mediastinum	0.90 (0.77-1.00)	0.56 (0.27-0.84)	0.19
Lung hilus	0.82 (0.65-0.99)	0.66 (0.39-0.92)	0.31
Abdomen	0.68 (0.42-0.93)	0.71 (0.43-0.99)	0.88
Pelvis	0.52 (0.15-0.89)	0.88 (0.74-1.00)	0.38
Groin	0.40 (0.02-0.78)	0.64 (0.31-0.98)	0.31
<i>Organs</i>	$\kappa_w$ (95% CI <sup>a</sup> )	$\kappa_w$ (95% CI)	<i>p</i> -value
Brain	0.79 (0.57-1.00)	0.49 (0.16-0.82)	1.00
Head (extra cerebral)	0.66 (0.64-0.68)	0.35 (0.04-0.65)	0.063
Throat	0.26 (0.13-0.65)	0.49 (0.26-0.82)	0.38
Lungs and pleural cavity	0.65 (0.38-0.91)	0.79 (0.56-1.00)	1.00
Mediastinum	0.49 (0.16-0.82)	0.32 (0.09-0.73)	1.00
Liver	0.81 (0.53-1.00)	0.90 (0.80-1.00)	1.00
Gall bladder	N/A <sup>b</sup>	N/A	N/A
Spleen	0.66 (0.64-0.66)	0.74 (0.43-1.00)	0.50
Kidneys	0.49 (0.16-0.82)	0.66 (0.64-0.68)	1.00
Adrenals	0.71 (0.41-1.00)	0.26 (0.13-0.65)	0.75
Pancreas	0.49 (0.16-0.82)	0.79 (0.59-1.00)	N/A
Internal genitals	0.38 (0.01-0.77)	0.65 (0.34-0.96)	0.63
Bladder	0.66 (0.65-0.67)	0.66 (0.64-0.66)	1.00
<i>Gastrointestinal tract</i>	$\kappa_w$ (95% CI <sup>a</sup> )	$\kappa_w$ (95% CI)	<i>p</i> -value
Oesophagus	N/A	N/A	N/A
Ventricle	0.66 (0.64-0.68)	0.79 (0.57-1.00)	1.00
Small intestine	0.49 (0.16-0.82)	0.56 (0.36-0.76)	1.00
Colon	0.79 (0.57-1.00)	0.73 (0.49-0.96)	<b>0.016</b>
Mesenterium	N/A	N/A	N/A
<i>Soft tissues</i>	$\kappa_w$ (95% CI <sup>a</sup> )	$\kappa_w$ (95% CI)	<i>p</i> -value
Throat	0.38 (0.01-0.77)	0.49 (0.16-0.82)	1.00
Thorax	0.65 (0.30-1.00)	0.75 (0.51-0.99)	0.63
Abdomen	0.49 (0.16-0.82)	0.51 (0.09-0.93)	0.25
Pelvis	0.55 (0.21-0.89)	0.43 (0.06-0.81)	0.063
Extremities	0.49 (0.16-0.82)	0.65 (0.42-0.88)	<b>0.002</b>
<i>Skeleton</i>	$\kappa_w$ (95% CI <sup>a</sup> )	$\kappa_w$ (95% CI)	<i>p</i> -value
Skull & face	0.66 (0.64-0.68)	0.49 (0.16-0.82)	1.00
Spine	0.69 (0.38-1.00)	0.58 (0.21-0.95)	1.00
Thorax	0.60 (0.26-0.93)	0.48 (0.12-0.85)	0.31
Pelvis	0.89 (0.74-1.00)	0.86 (0.68-1.00)	0.75
Extremities	0.49 (0.16-0.82)	0.32 (0.04-0.61)	<b>0.008</b>

<sup>a</sup>CI = confidence intervals; <sup>b</sup>N/A = not applicable; P values ≤ 0.05 were considered to be statistically significant. Bold p-values indicate statistically significant differences.



**Table 2** Histological findings (primary cancer) and the complimentary findings using whole-body MRI (WB-MRI) and <sup>18</sup>F-FDG-PET/CT (PET/CT).

Patient	Gender	Age	Histological findings	WB-MRI	PET/CT
1	♂	63	Lung cancer	+	+
2	♂	69	No malignancy		
3	♂	85	Prostate cancer	-	+
4	♂	73	Colangiocarcinoma	+	+
5	♂	77	No malignancy		
6	♀	58	No malignancy		
7	♂	58	No malignancy		
8	♀	81	No malignancy		
9	♀	73	Lung cancer	+	+
10	♀	69	No malignancy		
11	♂	69	Lung cancer	+	+
12	♂	34	Hodgkin's disease	+	+
13	♂	66	Prostate cancer	+/-*	-
14	♂	66	Renal cell carcinoma	-	-
15	♀	61	No Malignancy		
16	♂	66	Malignant lymphoma	+	+
17	♀	44	No Malignancy		
18	♂	65	No Malignancy		
19	♀	48	No Malignancy		
20	♂	74	Malignant melanoma	+	+
21	♂	51	No Malignancy		
22	♀	69	No Malignancy		
23	♂	48	No Malignancy		
24	♀	64	Lung cancer	+	+
25	♂	70	Malignant lymphoma	+	+

A positive sign (+) means that the suspicious lesions/<sup>18</sup>F-FDG avid foci were found by both raters; A negative sign (-) means that the malignancy was missed by both raters. Grey markings are patients with positive histological findings; 'No malignancy' indicates that neither of the modalities found any suspicious lesions/<sup>18</sup>F-FDG avid foci; Gender: ♀ = female; ♂ = male; \*In this patient, one WB-MRI rater found the lesion while the other missed it.

± 2.0 min respectively. The mean time spent for image evaluation was 119 ± 78 min for the MRI and 9 ± 4 min for the <sup>18</sup>F-FDG-PET/CT evaluation.

The total radiation dose for the <sup>18</sup>F-FDG-PET/CT examinations, used for this type of examination is (mSv ± standard deviation) 11.7±2.3 mSv (6.1 mSv from the low dose CT and 5.6 mSv from the <sup>18</sup>F-FDG injection). For radiation friendly screening purposes, the clinical value of Whole-Body MRI (WB-MRI) in detection of suspicious lesions is similar to avid foci detection in whole-body <sup>18</sup>F-FDG-PET/CT. The WB-MRI technique is slow and data analysis cumbersome compared to the applied nuclear imaging technique. However, the MRI approach could be feasible in vulnerable patient subgroups such as young patients, during pregnancy or dysregulated diabetics.

**Discussion**

Fair to strong interobserver reliability (weighted kappa values of 0.26 to 0.88-0.90) were found between each pair of specialists. In this context, kappa values cannot be

directly used to discriminate between random differences and systematic differences. Therefore, any disagreement caused by chance cannot be separated from any consistent pattern in the sampled data [19]. Larger disagreements (e.g. scale values 1 vs 4) lead to larger decreases in weighted kappa than slight disagreements (e.g. scale values 2 vs 3 or 3 vs 4). To this end, as much information as possible was derived from the data by analyzing these on the highest scale available, meaning the 4-point scale (in opposition to dichotomizing the scale into two categories 1 vs 2-4). Thus, the kappa values indicate that raters of both modalities do not always agree and the interobserver variability is approximately the same.

Our main finding was that there was no statistical difference between WB-MRI and <sup>18</sup>F-FDG-PET/CT in regard to the detection of suspicious lesions and <sup>18</sup>F-FDG avid foci in 32 out of 35 unique anatomical regions including the lymph nodes, the organ systems, gastrointestinal tract, the soft tissues of the trunk and the skeleton. Figure 1 shows an example of the two modalities with converging findings in a patient with malignant disease in the liver and the lungs. These findings seem to indicate that WB-MRI can be used as an alternative non-ionizing screening tool and is supported by the findings of Stecco et al. [20] who underlined the usefulness of WB-MRI for cancer screening, staging and follow-up.

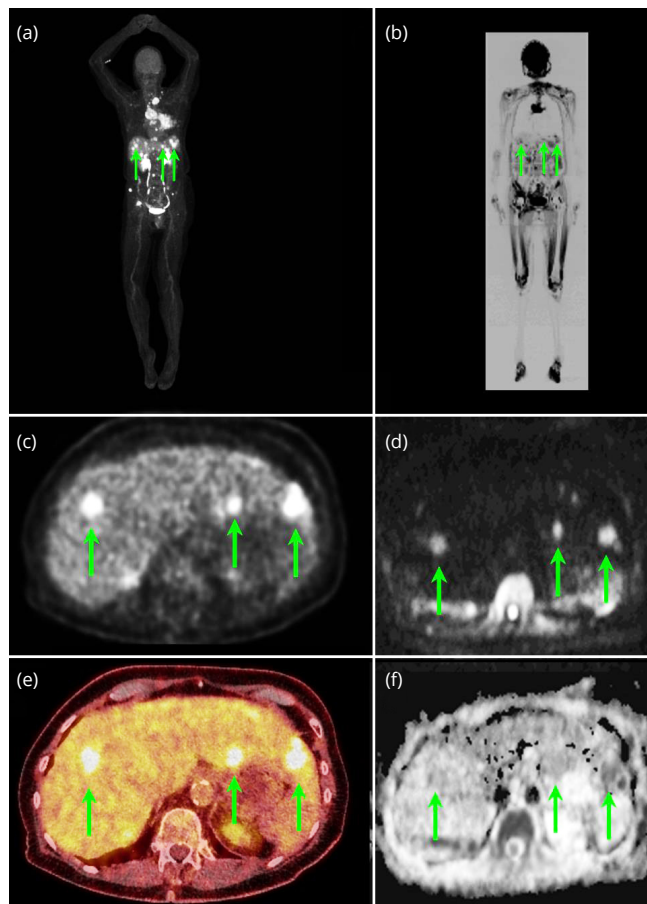


**Figure 1** Example of a patient with coincidence of suspicious lesions/<sup>18</sup>F-FDG avid foci in the liver and lungs using <sup>18</sup>F-FDG-PET/CT and diffusion weighted MRI. (a) 3D whole-body <sup>18</sup>F-FDG-PET/CT scan, (b) 3D Diffusion Weighted Whole-body Imaging with Background Body Signal Suppression (DWIBS), (c) axial <sup>18</sup>F-FDG-PET slice of the liver, (d) axial DWI slice with a b-value of 900, (e) merged <sup>18</sup>F-FDG-PET/CT and (f) is an axial ADC map.

A statistically significant difference between the two modalities was, among others, found in the colon ( $p = 0.016$ ). Figure 2 shows an example of a patient with an  $^{18}\text{F}$ -FDG avid focus in the colon while the MRI examination found no noticeable pathology. The nuclear medicine physicians noted that their findings may be physiologic in origin and therefore possibly benign. In comparison, the suspicious lesion found on the DWI images ( $b=900 \text{ s/mm}^2$ ) had no ADC correlation and therefore the MRI radiologists noted the finding as benign. In this particular case, the suspicious lesions were most likely caused by a  $T_2$ -shine-through effect and therefore not marked as a suspicious on the MRI scan. Nevertheless, as no biopsy was carried out for the specific lesion, it can only be stated that the two modalities differ in this particular case and not which modality were actually right.

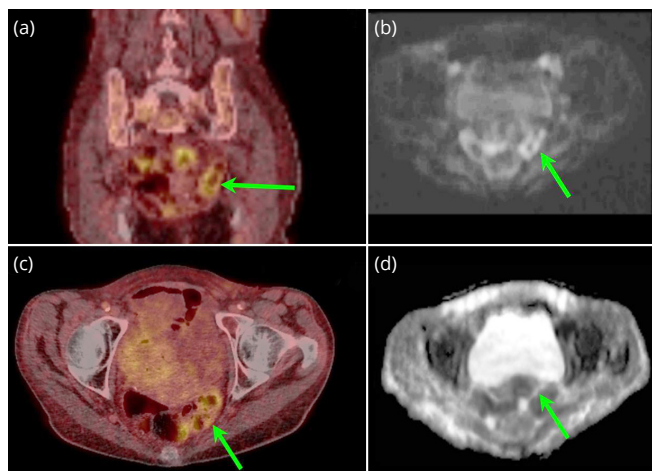


**Figure 2** Example of a patient with  $^{18}\text{F}$ -FDG avid foci found in the colon while the MRI examination found no noticeable pathology. Green arrows point to the specific anatomical area of interest of the sigmoid in the lower left side of the abdomen. (a and c) Axial and coronal slice planes from the  $^{18}\text{F}$ -FDG-PET/CT. (b) Axial image from the Whole-body MRI diffusion sequence ( $b=900 \text{ s/mm}^2$ ). (d) Corresponding ADC map. The diffusion weighted MRI images indicated that the suspicious lesion was a  $T_2$ -shine-through effect and therefore not malignant.

Statistically significant differences between the two modalities were also found in the soft tissue of the extremities ( $p = 0.002$ ). A total of ten patients had  $^{18}\text{F}$ -FDG avid foci, while only one patient had a single suspicious lesion identified using WB-MRI. The  $^{18}\text{F}$ -FDG-PET/CT findings included tissue in the proximity of the humerus, the knees, the feet and the skin of the extremities. The discrepancy between the findings may have several origins. Firstly, the arms of the patients were placed in the outer rims of the magnetic field of view causing a clear visual reduction in image quality (lower Signal to Noise and contrast). Secondly, images of the legs were carried out using MRI coils which are not optimized for imaging the limbs as e.g. dedicated knee or foot coils are. Thus, in several cases, the area with positive findings by the nuclear technique was either poorly imaged (e.g. noisy images or lacked contrast) or even missing from the MRI data due to the physical placement on the rim of the signal sensitive parts of the MRI receive coils. Acquiring data from these areas more sufficiently with MRI, the total scan time would have to be extended. Even though it seems unlikely, the  $^{18}\text{F}$ -FDG-PET/CT may have yielded false positive lesions. Hence, as there are no biopsy reports from these areas, it can only

be stated that the two modalities differ. Figure 3 shows an example of the issue.

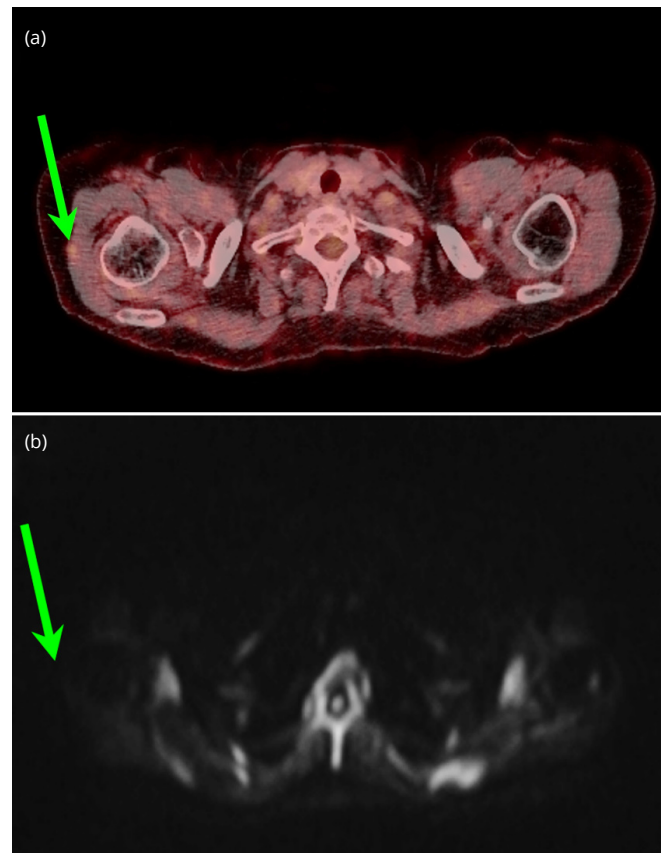


**Figure 3** Example of a patient with an  $^{18}\text{F}$ -FDG avid focus in the soft tissue of the right arm while the MRI examination found no noticeable pathology. (a) Axial  $^{18}\text{F}$ -FDG-PET/CT image. The green arrow points to the area of an  $^{18}\text{F}$ -FDG avid focus. (b) Axial diffusion weighted MRI ( $b = 900 \text{ s/mm}^2$ ) of the same image slice, but without any hyperintensity. The reduction in MRI signal intensity was caused by the location of the anatomy on the outer rims of the field of view.

Finally, statistically significant differences were seen between lesions in the skeleton of the extremities ( $p = 0.008$ ). In this case, the  $^{18}\text{F}$ -FDG-PET/CT technique found eight patients with  $^{18}\text{F}$ -FDG avid foci in the skeleton while MRI found one with a suspicious lesion. The differences can again, in part, be explained by the poor image quality of the extremities using MRI.

Based on our findings, we do not recommend that future WB-MRI protocols for screening purposes include the extremities as the images are of a non-diagnostic quality. Furthermore, withdrawal of the extremities from the imaging protocols will reduce the total MRI scan time substantially. The same may hold true at higher magnetic field strengths. The next step, if any suspicious lesion is identified, is to carry out dedicated MRI protocols targeted at the suspected pathology.

Comparing the findings of the two modalities and the histological tests, three cases exhibited discrepancies between the modalities as evident from Table 2. Histological evidence indicated that two of these patients had prostate cancer (Patient #3 and #13). One of them was identified by  $^{18}\text{F}$ -FDG-PET/CT and not by WB-MRI while the other was identified by only one of the MRI radiologists

and neither of the nuclear physicians. It is well-known that many prostate cancers do not present with increased  $^{18}\text{F}$ -FDG uptake and therefore  $^{18}\text{F}$ -FDG-PET/CT is not part of the prostate cancer staging routine. In regards to MRI, the setup of the MRI screening protocol is limited by several factors. The combination of a higher b-value (1,500-2,000s/mm<sup>2</sup>) and the addition of a T<sub>2</sub>-weighted sequence may have provided a more sensitive tumor detection [21]. It should be noted that using a contrast agent for tumor detection may not have added to the detection of the cancer as there is an overlap in enhancement patterns with prostatitis and benign prostate hyperplasia nodules [22]. Finally, optimizing the detection of malignant disease in the prostate also calls for a dedicated coil (e.g. an endorectal coil). We applied a larger body coil as part of the WB-MRI screening setup.

Both modalities missed a renal cell carcinoma (Patient#14). The patient had a large cystic tumor on the lower pole of the left kidney.  $^{18}\text{F}$ -FDG activity was present in the periphery of the tumor but was interpreted as physiological FDG-excretion in the urine. In general, physiological  $^{18}\text{F}$ -FDG in the urine hampers the assessment of urinary system abnormalities. On the MRI scans, it is well-known that renal cell carcinoma is not well seen and cystic changes are often challenged by T<sub>2</sub>-shine through effects. In this context, Galia et al. [23] pointed out that the detection of renal cell carcinoma can be challenging also in non-cystic lesions since it poorly uptakes  $^{18}\text{F}$ -FDG and can show no restricted pattern of diffusion. In their work, they reported a case of renal cell carcinoma missed by PET and whole body DWI but detected by post-contrast MRI images. Thus, using contrast enhanced MRI may have contributed to the detection of the tumor while diffusion weighted imaging still needs to be further evaluated [24].

The two scan techniques yielded similar preparation times of approximately 10-13 min. However, the total scan time varied between the two modalities. MRI is a rather time-consuming modality compared to other imaging techniques. The average active MRI scan time of 75 min is more than twice as long compared to the nuclear modality of approximately 32 min and also about the maximum time a patient can withstand to be inside the MRI scanner bore. In this perspective,  $^{18}\text{F}$ -FDG-PET/CT is much more patient friendly as the entire scan session can be completed within approximately half an hour.

The time the observers spent for image evaluation varied vastly between the two modalities. The nuclear medicine physicians spend in average less than 9 min for evaluation while the MRI radiologists spend in average 75 and 162 min respectively. The large discrepancy can in part be found in the way the images were evaluated. The nuclear physicians only registered the time it took to systematically look through the images and detect the number and anatomical localization of  $^{18}\text{F}$ -FDG avid foci. Thus, the noted time does not represent a full clinical evaluation. The radiologists on the other hand registered the gross time they spent including the clinical evaluation of each patient. Regardless of how the evaluation times were noted, the difference clearly shows that WB-MRI is more time-consuming, not only the acquisition time, but also the image evaluation.

The average radiation exposure from an  $^{18}\text{F}$ -FDG-PET/CT examination is on average 11.7 mSv. This value is based on a low dose CT scan from the  $^{18}\text{F}$ -FDG-PET/CT scan as a full dose diagnostic CT scan had already been obtained at the referring hospital as part of the initial diagnosing. MRI does not expose the patient to any ionizing radiation and this is a major advantage of this modality and the argument for MRI's superiority in radiation-sensitive patients, e.g. children and pregnant women. As the majority of patients suspected of malignant disease are older this issue is of minor importance. Like  $^{18}\text{F}$ -FDG-PET/CT, WB-MRI protocol does not require the use of a contrast agent making both modalities for patients with reduced renal function to reduce the risk of Nephrogenic systemic fibrosis [25].

The study has a clear limitation as only about half of the patients had a malignant disease and that not all suspicious lesions could be verified by biopsy.

## Conclusion

A WB-MRI examination using dedicated DWI sequences at a field strength of 1.5T detects suspicious lesions similar to FDG-PET/CT. However, the MRI technique is slow and data analysis cumbersome compared to the applied nuclear imaging technique. Nevertheless, for determining the presence of malignancy or other pathology, WB-MRI could be an alternative non-ionizing modality to standard whole-body  $^{18}\text{F}$ -FDG-PET/CT in vulnerable patient subgroups such as young patients, during pregnancy or dysregulated diabetics.

## Ethics committee approval

The project was approved by The Central Denmark Region Committees on Health Research Ethics, case no. 1-10-72-381-13 and reported to the Danish Data Protection Agency.

## Acknowledgement

The authors would like to thank the Department of Biostatistics, Institute of Public Health, Health, Aarhus University, Denmark, for their consultancy services in statistics and research methodology.

## Funds

The project was supported by the Regional Hospital Central Jutland Research Fund (Hospitalsenhed Midts forskningspulje), grant no. 634926.

## Conflicts of interest

The authors have no conflicts of interest

## References

- [1] Xu H, Zhang M, Zhai G, Li B. The clinical significance of  $^{18}\text{F}$ -FDG-PET/CT in early detection of second primary malignancy in cancer patients. *J Cancer Res Clin Oncol*. 2010; 136(8):1125-1134.
- [2] Poeppel TD, Krause BJ, Heusner TA, Boy C, Bockisch A, et al. PET/CT for the staging and follow-up of patients with malignancies. *Eur J Radiol*. 2009; 70(3):382-392.
- [3] Ferda J, Ferdova E, Zahlava J, Walter J, Mukensnabl P, et al. ( $^{18}\text{F}$ -FDG-PET/CT of orofacial tumors, a value of whole-body imaging approach. *Eur J Radiol*. 2010; 73(2):241-248.

- [4] Kleiner S, Weber W. Importance of FDG-PET/computed tomography in colorectal cancer. *Radiologe*. 2019; 59(9):812-819.
- [5] Facey K, Bradbury I, Laking G, Payne E. Overview of the clinical effectiveness of positron emission tomography imaging in selected cancers. *Health Technol Assess*. 2007; 11(44):iii-267.
- [6] Wachsmann JW, Gerbaudo VH. Thorax: normal and benign pathologic patterns in FDG-PET/CT imaging. *PET Clin*. 2014; 9(2):147-168.
- [7] Long NM, Smith CS. Causes and imaging features of false positives and false negatives on F-PET/CT in oncologic imaging. *Insights Imaging*. 2011; 2(6):679-698.
- [8] Petralia G, Padhani A, Summers P, Alessi S, Raimondi S, et al. Whole-body diffusion-weighted imaging: is it all we need for detecting metastases in melanoma patients? *Eur Radiol*. 2013; 23(12):3466-3476.
- [9] Stephane V, Samuel B, Vincent D, Joelle G, Remy P, et al. Comparison of PET-CT and magnetic resonance diffusion weighted imaging with body suppression (DWIBS) for initial staging of malignant lymphomas. *Eur J Radiol*. 2013; 82(11):2011-2017.
- [10] Padhani AR, Tunariu N. Metastasis reporting and data system for prostate cancer in practice. *Magn Reson Imaging Clin N Am*. 2018; 26(4):527-542.
- [11] Tarnoki DL, Tarnoki AD, Richter A, Karlinger K, Berczi V, et al. Clinical value of whole-body magnetic resonance imaging in health screening of general adult population. *Radiol Oncol*. 2015; 49(1):10-16.
- [12] Morone M, Bali MA, Tunariu N, Messiou C, Blackledge M, et al. Whole-Body MRI: Current applications in oncology. *AJR Am J Roentgenol*. 2017; 209(6):W336-W349.
- [13] Purandare NC. Inclusion of brain in FDG PET/CT scanning techniques in cancer patients: Does it obviate the need for dedicated brain imaging? *Indian J Nucl Med*. 2011; 26(2):64-66.
- [14] Padhani AR, Koh DM, Collins DJ. Whole-body diffusion-weighted MR imaging in cancer: current status and research directions. *Radiology*. 2011; 261(3):700-718.
- [15] Kottner J, Audige L, Brorson S, Donner A, Gajewski BJ, et al. Guidelines for reporting reliability and agreement studies (GRRAS) were proposed. *J Clin Epidemiol*. 2011; 64(1):96-106.
- [16] Cicchetti D AT. A new procedure for assessing reliability of scoring EEG sleep recordings. *AMER J EEG Technol*. 1971; 11(3):101-110.
- [17] Landis JR, Koch GG. The measurement of observer agreement for categorical data. *Biometrics*. 1977; 33(1):159-174.
- [18] Newcombe RG AD. Proportions and their differences. In: *Statistics with confidence, Second edition edn* (ed. Altman DG, M. D., Bryant TN, Gardner MJ) (2000), pp. 45-56.
- [19] Mandrekar JN. Measures of interrater agreement. *J Thorac Oncol*. 2011; 6(1):6-7.
- [20] Stecco A, Romano G, Negru M, Volpe D, Saponaro A, et al. Whole-body diffusion-weighted magnetic resonance imaging in the staging of oncological patients: comparison with positron emission tomography computed tomography (PET-CT) in a pilot study. *Radiol Med*. 2009; 114(1):1-17.
- [21] Maurer MH, Heverhagen JT. Diffusion weighted imaging of the prostate-principles, application, and advances. *Translational andrology and urology*. 2017; 6(3):490-498.
- [22] Fusco R, Sansone M, Granata V, Setola SV, Petrillo A. A systematic review on multiparametric MR imaging in prostate cancer detection. *Infectious agents and cancer*. 2017; 12:57.
- [23] Galia M, Albano D, Bruno A, Agrusa A, Romano G, et al. Imaging features of solid renal masses. *Br J Radiol*. 2017; 90(1077):20170077.
- [24] Chiarello MA, Mali RD, Kang SK. Diagnostic accuracy of MRI for detection of papillary renal cell carcinoma: A systematic review and meta-analysis. *AJR Am J Roentgenol*. 2018; 211(4):812-821.
- [25] Thomsen HS. Nephrogenic systemic fibrosis: history and epidemiology. *Radiol Clin North Am*. 2009; 47(5):827-831.